Homodyne-detector-blinding attack in continuous-variable quantum key distribution

Hao Qin,[1,2,3,4,5,*] Rupesh Kumar,[5,6] Vadim Makarov,[7,3] and Romain Alléaume[5]

[1]*Institute for Quantum Computing, University of Waterloo, Waterloo, Ontario, Canada N2L 3G1*
[2]*Department of Combinatorics and Optimization, University of Waterloo, Waterloo, Ontario, Canada N2L 3G1*
[3]*Department of Physics and Astronomy, University of Waterloo, Waterloo, Ontario, Canada N2L 3G1*
[4]*CAS Quantum Network Co., Ltd., 99 Xiupu Road, Shanghai 201315, People's Republic of China*[†]
[5]*Télécom ParisTech, LTCI, 46 Rue Barrault, 75634 Paris Cedex 13, France*
[6]*Department of Physics, University of York, York YO10 5DD, United Kingdom*[†]
[7]*Russian Quantum Center and MISIS University, Moscow, Russia*

We propose an efficient strategy to attack a continuous-variable (CV) quantum key distribution (QKD) system, which we call homodyne detector blinding. This attack strategy takes advantage of a generic vulnerability of homodyne receivers: A bright light pulse sent on the signal port can lead to a saturation of the detector electronics. While detector saturation has already been proposed to attack CV QKD, the attack we study in this paper has the additional advantage of not requiring an eavesdropper to be phase locked with the homodyne receiver. We show that under certain conditions, an attacker can use a simple laser, incoherent with the homodyne receiver, to generate bright pulses and bias the excess noise to arbitrary small values, fully comprising CV QKD security. These results highlight the feasibility and the impact of the detector-blinding attack. We finally discuss how to design countermeasures in order to protect against this attack.

I. INTRODUCTION

Quantum key distribution (QKD) [1,2] is one of the most important and practical applications of quantum information processing. It has already been made commercially available and has been deployed in test and production environments. Quantum key distribution allows two remote parties, Alice and Bob, to establish a secret key over a public quantum channel, assisted by a classical communication channel. Quantum key distribution security can notably be guaranteed even against computationally unbounded adversaries, making QKD the only available information-theoretic secure key establishment scheme practically available to date, beyond the use of physically protected secret couriers. Quantum key distribution information-theoretic security, however, relies on some minimal set of assumptions: Alice's and Bob's laboratories, where secret information is stored and processed, should not leak this information to the outside world; moreover, Alice's and Bob's hardware (laser, modulators, and detectors) is supposed to behave (at least approximately) according to an abstracted model that then allows one to prove theoretical security. However, in practice, the real-world QKD implementations do not exactly verify the aforementioned assumptions and such deviations may lead to vulnerabilities and enable an eavesdropper, Eve, to launch so-called side channel attacks and break the security of practical QKD devices.

In discrete-variable (DV) QKD, the single-photon detector (SPD) is the most exposed device, from the implementation

security viewpoint, and several attack strategies have been proposed to exploit SPD vulnerabilities and attack DV QKD implementations. Attacks such as time shift [3,4], after gate [5], blinding [6], and spatial mode mismatch [7] attacks may all lead to security breach. Among those attacks, the blinding attack is probably considered the most powerful attack, as this attack strategy allows Eve to actively control Bob's SPD remotely, using intense light. Such a kind of attack has been experimentally demonstrated on commercial QKD systems [8] and in a full-field deployment [9]. Various countermeasures [10,11] have been proposed against detector-based attacks. However, only measurement-device-independent (MDI) QKD [12,13], i.e., QKD protocols where security can be established without trusting the detector, can be firmly demonstrated to be immune against these attacks targeting SPDs.

Continuous-variable QKD [14] is another promising approach to perform quantum key distribution. It relies on continuous modulation of the light field quadratures and measurements with coherent detection (homodyne or heterodyne detectors) instead of SPDs in DV QKD systems. Benefiting from coherent detection, CV QKD can be fully implemented with off-the-shelf optical communication components [15–17]. Moreover, the local oscillator (LO) in the coherent detection acts as a built-in filter to efficiently remove any noise photons in different modes, which enable CV QKD to be deployed in coexistence with intense classical channels over optical networks [18] and to be possibly implemented in daylight free-space environments. Continuous-variable QKD practical implementations, however, also suffer from potential vulnerabilities. For example, LO manipulation is a long-standing security problem: If the LO is sent on the public channel, then an attacker can modify LO pulses in different ways [19–23]

*qinhao@casquantumnet.com
†Present address.

and learn secret keys without being discovered. A generic solution to this issue, however, has been recently proposed: locally generated LO (LLO) pulses on Bob's side [24–27]. Regarding the homodyne detection (HD), which is a central component in CV QKD, it has been shown in [28,29], under the name saturation attack, that HD saturation can be induced by an attacker and exploited to launch attacks that can fully break CV QKD security. More precisely, it has been shown that HD saturation induced by a coherent displacement can bias the excess noise estimation and conceal the presence of an eavesdropper, performing an intercept-resend attack on the signals sent by Alice. However, coherently displacing the signal sent by Alice, without adding detectable excess noise, is highly challenging, making this attack strategy difficult to implement in practice.

In this paper, inspired by the blinding attack in DV QKD, we propose a simple and practical way to saturate a homodyne detector with a finite linear detection range. The attack exploits the loss imbalance of the two ports in a balanced homodyne detector and consists in sending a bright pulse onto the signal port to induce electronic saturation. Such a loss imbalance is quite generic to any homodyne detector implementation: The two photodiodes quantum efficiencies as well as the beam-splitter reflection and transmittance coefficients are never perfectly balanced. This implies the need for additional balancing, which is in general ensured by introducing some variable attenuation in one of the optical arms. Such balancing must be done with precision with respect to the LO port, since LO pulses are intense. However, as a consequence, a good balancing in practice cannot, in return, be guaranteed with respect to the other port, i.e., the signal port. As a consequence, any relatively strong light impinging on the signal port will produce a comparatively stronger photocurrent on one of the homodyne detector photodetectors, which will further cause homodyne detector's amplifier electronic saturation.

Due to HD saturation, Bob's HD output signals are limited within some finite range. This however violates a basic assumption generally used in CV QKD security proof: linearity, namely, that Bob's HD output signal is supposed to be linearly proportional to the input optical quadratures. The principle of the blinding attack we introduce here consists, for Eve, in actively driving Bob's homodyne detector into a saturated response mode, by sending strong external pulses on the signal port. We will show that such manipulation can be used to reduce the estimated excess noise, under certain conditions. More precisely, we will show that by combining the sending of strong light pulses to Bob with a full intercept-resend attack, Eve can break the security of the widely used Gaussian modulated coherent state (GMCS) CV QKD protocol [30,31]. We will analyze the conditions such that Eve can achieve a full security break, illustrating that this attack can be implemented with current technologies and a low-complexity experimental system. Importantly, our attack only targets the HD, which means even the recently proposed LLO CV QKD scheme is not immune to this attack if no countermeasure is considered. This highlights that detector loopholes also exist in CV QKD and can potentially affect all CV QKD implementations. Finally, we will discuss possible countermeasures against detector-based attacks in CV QKD and compare them with countermeasures against blinding attack in DV QKD.

This paper is organized as follows. In Sec. II we present the security basis of GMCS CV QKD: parameter estimation and its relation to quantum hacking. In Sec. III we study experimentally several imperfections of a practical homodyne detector and predict the shot-noise measurements with the proposed HD model. In Sec. IV we introduce the attack strategy of the homodyne detector-blinding attack. In Sec. V we perform the security analysis of the proposed strategy and demonstrate its security breach feasibility in simulations. We discuss possible countermeasures against HD-blinding attack in CV QKD in Sec. VI. We summarize in Sec. VII.

II. PRACTICAL SECURITY IN CV QKD

In this section we briefly present the GMCS CV QKD protocol. This protocol is widely used, notably due to a well-understood security proof, based on the optimality of Gaussian attacks [32]. We will be focused on the GMCS protocol throughout the paper and illustrate in this section the connection between the parameter estimation phase and the practical attack strategy.

A. The GMCS protocol and parameter estimation

In the GMCS protocol [30], Alice prepares the coherent state $|X + iP\rangle$ as the quantum signal in which amplitude X and phase P quadratures are continuously modulated with a centered Gaussian distribution with a variance $V_A N_0$. The shot noise N_0 is the HD variance when the input signal is in a vacuum field. On Bob's side, he performs HD on Alice's signal by interfering with it using a strong phase reference LO. Bob randomly chooses to apply a phase modulation 0 or $\pi/2$ on the LO in order to measure the quadrature X or P in phase space. Note that it is not necessary for Alice to send the LO over the insecure channel; Bob can generate the LO on his side and recover the phase information with the help of additional reference pulses from Alice [24–27]. By repeating such a process and sifting, Alice and Bob then obtain correlated Gaussian variables X_A and X_B as the raw keys. With reverse reconciliation [30,33], Alice and Bob can extract an identical bit string from the correlated variables and obtain a secret key through privacy amplification.

In order to estimate Eve's knowledge about the raw key and eliminate it in privacy amplification, an important step for Alice and Bob is to perform the parameter estimation to estimate excess noise, channel transmission, and secret key rate. Security proofs of CV QKD show that the Gaussian attack is the optimal one which has been proven in collective attacks with an asymptotic limit [34,35], in a recent composable security proof [36], and in arbitrary attacks with finite size [37]. Such security proofs enable Alice and Bob to describe their quantum channel as a Gaussian linear channel which connects the raw data X_A and X_B with a Gaussian noise factor X_N. This channel model allows Alice and Bob to determine the two characteristics of the quantum channel, excess noise ξ and channel transmission T, by performing four measurements. In particular, Alice's modulation variance V_A, Bob's HD variance V_B, the Alice-Bob covariance Cov_{AB}, and the shot-noise calibration of Bob's HD variance $V_{B,0}$ when there is only LO

input

$$V_A = \langle X_A^2 \rangle - \langle X_A \rangle^2, \tag{1}$$

$$\text{Cov}_{AB} = \langle X_A X_B \rangle - \langle X_A \rangle \langle X_B \rangle = \sqrt{\eta T} V_A, \tag{2}$$

$$V_B = \langle X_B^2 \rangle - \langle X_B \rangle^2 = \eta T V_A + N_0 + \eta T \xi + v_{\text{ele}}, \tag{3}$$

$$V_{B_0} = N_0 + v_{\text{ele}}, \tag{4}$$

in which η and v_{ele} are Bob's HD overall efficiency and electronic noise which are calibrated before QKD, respectively, and N_0 is the shot-noise variance. Alice and Bob can extract a portion of the raw key and estimate the channel transmission T based on Eqs. 1 and 2 excess noise in shot-noise units ξ / N_0 based on Eqs. (3) and (4). They can then estimate the security key rate with a given security proof and decide whether to proceed to the key generation step or abort the protocol if there the secure key rate estimation is nonpositive. Note that we need to take statistical fluctuation into account for the variance measurements with a realistic data block size N [38] in practice. In this paper we want to emphasize the idea of the attack strategy; we only consider the collective attacks in the asymptotic limit ($N \to \infty$).

B. Quantum hacking in CV QKD

The goal of Eve's quantum hacking on the CV QKD system is to steal Alice's and Bob's secret keys without being discovered. To achieve this, Eve is allowed to use every possible measure that is allowed by quantum mechanics to attack the open quantum channel. Some CV QKD quantum hacking strategies such as wavelength attack [22] and LO intensity fluctuation attack [20] are only possible under the theory that Eve has full access to a future quantum computer with enough quantum memory. Under such cases, loopholes lead to an increase of Eve's mutual information with Alice or Bob and to a decrease of the final secret key rate. It is however more important to study possible quantum hacking strategies in a realistic scenario when Eve's power is limited by current technologies, as it would bring immediate threats to CV QKD security.

In CV QKD, excess noise estimation is the reference for Alice and Bob to decide to abort the protocol or proceed to key generation. Any flaw in the excess noise estimation can lead to the security problem that Eve's attack action is undiscovered, which may fully compromise CV QKD security. In order to attack CV QKD with current technologies, Eve can perform an intercept-resend (IR) attack by using optical heterodyne detection [39] which corresponds to an entanglement breaking channel. Under an IR attack, Eve always has an information advantage over Alice and Bob but she also introduces at least $2N_0$ into their excess noise estimation due to the heterodyne measurement disturbance and coherent state shot noise. Meanwhile, Eve can take advantage of CV QKD implementation imperfections to formalize particular attack strategies to bias Alice's and Bob's excess noise estimations in order to hide her IR action and achieve a full security breach. For example, in a calibration attack [19], Eve delays the LO pulse such that Alice and Bob overestimate the shot noise based on their preestablished calibration, which results

in underestimation of the excess noise. In a saturation attack [28,29], Eve induces saturation on Bob's HD measurement and directly biases Alice's and Bob's excess noise. In this paper we also follow this idea and will take advantage of several imperfections in HD to archive a security breach of GMCS CV QKD implementations.

III. IMPERFECT HOMODYNE DETECTION IN CV QKD

In this section we analyze HD imperfections such as imbalance and electronics saturation. These HD imperfections are the key elements that will be used in the homodyne detector-blinding attack strategy.

A. Practical homodyne detection with imperfections

In the context of CV QKD, HD performance is usually measured by its overall efficiency η and its electronic noise v_{ele} [15,17]. However, imperfections such as limited bandwidth, linearity range, and imperfect balance can also affect HD behavior and potentially impact the CV QKD performance [40]. Some of these HD imperfections may even open security loopholes in CV QKD to Eve which need to be carefully studied. Here we are particularly interested in the imperfection of the HD on the optical part, an imbalanced 50:50 beam splitter (BS), and on the electronic part, a finite linear range of detection.

As shown in Fig. 1, a practical homodyne detector consists of both optical and electronic parts. The input optical signals and LO pulses go into the two ports of the 50:50 BS and interfere with one another. Two output optical pulses then travel to two identical *p-i-n* photodiodes (PDs) which convert optical light into two photocurrents with finite quantum efficiencies. An electronic subtraction is then performed on the two photocurrents and the subtracted photocurrent is amplified in a small voltage through a transimpedance amplifier or a charge amplifier. The voltage signal is further amplified by a second stage amplifier to be detected by the analog-to-digital converter (ADC) device (i.e., oscilloscope or data acquisition card). The final digitized data are the so-called HD output signal which is proportional to the input optical quadratures. The selection of the quadrature is dependent on the relative phase between the LO and signal pulse.

Due to the subtraction of HD, most LO intensities are eliminated while the rest of the energy carries the small quantum signal fluctuation which is amplified by LO's amplitude. However, due to the imbalance imperfection of the HD, a non-negligible leakage of the LO contributes to the final HD output signal as an offset. Such leakage may also contribute LO intensity fluctuation noise to HD measurements if the LO
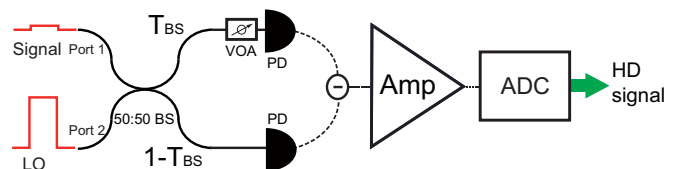

FIG. 1. Simplified scheme of a practical homodyne detector: BS, beam splitter; VOA, variable optical attenuator; PD, photodiode; Amp, amplifier; ADC, analog-to-digital converter; solid line, optical signal; dash line, electronic signal.

intensity is relatively high [41]. In order to adjust the balance of HD, a variable optical attenuator and a variable delay line need to be added to one of the optical paths after the 50:50 BS. The balancing of HD is evaluated by the common-mode rejection ratio (CMRR) $\mathcal{C}$, which is defined as $\mathcal{C} = -20\log_{10}(2\epsilon)$, with ϵ the overall imbalance factor [41]; ϵ quantifies the small deviation that varies from a perfectly balanced HD. For example, a typical CMRR value of a well-balanced HD is around -52.4 dB [40], which means the difference between the two photocurrents before subtraction is $\epsilon = 0.12\%$ over their total currents.

In order to quantify the impact of such an imbalance imperfection on HD, we analyze the case of shot-noise measurement when there is no signal but only LO pulses sent into HD, in which we look at the first and second moments of HD statistics: mean and variance. To simplify the analysis, we consider the model of unbalanced HD with two ports in Ref. [21]. If there is only a LO impinging on HD, the HD output state X_{HD} can be given by

$$X_{\mathrm{HD}} = \eta(1 - 2T_{\mathrm{HD}})I_{\mathrm{LO}} + 2\sqrt{\eta T_{\mathrm{HD}}(1 - T_{\mathrm{HD}})I_{\mathrm{LO}}}X_0 + X_{\mathrm{ele}}, \tag{5}$$

in which T_{HD} is the overall transmission of HD, which includes the transmission of the 50:50 BS, optical loss in the optical path, and efficiency of the PD, while $1 - T_{\mathrm{HD}}$ is the overall reflection and $\epsilon = 1 - 2T_{\mathrm{HD}}$ is thus the overall imbalance factor. In addition, I_{LO} is the number of photons per one LO pulse (which is linearly dependent on LO power or intensity), X_0 is the vacuum state, and X_{ele} is the homodyne detector electronic noise with a variance of v_{ele}. We observe that the HD output is displaced by a value D_{LO} [first term in Eq. (5)] that is linearly proportional to I_{LO} due to LO leakage, which directly determine the mean of X_{HD},

$$\langle X_{\mathrm{HD}} \rangle = D_{\mathrm{LO}} = \eta(1 - 2T_{\mathrm{HD}})I_{\mathrm{LO}}, \tag{6}$$

where the vacuum state is centered on zero $\langle X_0 \rangle = 0$ and we assume the offset due to the homodyne detector electronics is small enough to be neglected $\langle X_{\mathrm{ele}} \rangle \approx 0$. We can further deduce the HD variance based on Eq. (5) with the definition of variance

$$\begin{aligned} V_{\mathrm{HD}} &= \langle X_{\mathrm{HD}}^2 \rangle - \langle X_{\mathrm{HD}} \rangle^2 \\ &= \eta^2(1 - 2T_{\mathrm{HD}})^2 f_{\mathrm{LO}}^2 I_{\mathrm{LO}}^2 + 4(1 - T_{\mathrm{HD}})T_{\mathrm{HD}}\eta I_{\mathrm{LO}} \\ &\quad + v_{\mathrm{ele}}, \end{aligned} \tag{7}$$

in which $f_{\mathrm{LO}} = \sqrt{\langle I_{\mathrm{LO}}^2 \rangle - \langle I_{\mathrm{LO}} \rangle^2}/I_{\mathrm{LO}}$ is the intensity fluctuation ratio of LO over the measurement time and the first quadratic term of I_{LO} is the noise variance due to LO intensity fluctuations [41]. If we consider a typical CV QKD implementation [17] with a low LO power I_{LO} as the order of 10^8 and HD is adjusted to be balanced ($T_{\mathrm{HD}} \approx 0.5$), we can neglect the LO intensity fluctuation noise and the degradation effect due to imbalance as the factor $4(1 - T_{\mathrm{HD}})T_{\mathrm{HD}} \approx 1$. Equation (7) can be further simplified into

$$V_{\mathrm{HD}} \approx \eta I_{\mathrm{LO}} + v_{\mathrm{ele}}, \tag{8}$$

where the first term is known as the shot noise $N_0 = \eta I_{\mathrm{LO}}$ in CV QKD, which is proportional to I_{LO} and can be interpreted as the HD signal variation due to interference between the LO

and the vacuum state with $\langle X_0^2 \rangle = 1$. The amplification of the LO also applies to the vacuum state, which is attributed to the term of I_{LO} in Eq. (8). As shown in Eqs. (5) and 7, LO leakage due to HD imbalance contributes an offset of D_{LO} in HD output signals and associated LO intensity noises in the HD variance measurement.

Besides the HD imbalance imperfection, the finite linear detection range of the electronic part can also influence HD measurements and may lead to security loopholes [28,29]. An important assumption in CV QKD is that Bob's HD measurement varies linearly with the input optical quadrature. However, such an assumption does not always hold in a practical HD, because if the input field quadrature exceeds a certain threshold, the corresponding photocurrent would be relatively large, which can saturate the electronics and results in saturation of the HD output signal. Electronic saturations usually happen on the amplifier or on the data acquisition (DAQ) card. Depending on the specific electronic design, the amplifiers usually saturate at a few volts, which is an intrinsic characteristic of the electronics. The DAQ detection range in CV QKD is usually set to a small range (typically between -1 and 1 V) to ensure its measurement step precision; in principle, this range can be set as large as possible but not infinite. However, the overall linear detection range is still limited by the amplifier. Two p-i-n PDs in HD can also become saturated mainly due to screening of the electric field caused by photogenerated carriers [42]. However, such a limit is often relatively high (e.g., a few milliwatts for Thorlabs FGA01FC) and the total optical power of the LO and signal in the CV QKD system is much lower than this limit. Thus PD saturation is usually not the cause of HD saturation and we consider this realistic assumption in this paper. In practice, HD saturation is unavoidable and it is important to make sure that homodyne detector works in the linear region. The HD saturation effect can be modeled by a simple HD model [28,29] with upper and lower bounds α_1 and α_2, where Bob's HD output signal after the ADC can be given as

$$X_{\mathrm{HD_r}} = \begin{cases} \alpha_1, & X_{\mathrm{HD}} \geqslant \alpha_1 \\ X_{\mathrm{HD}}, & \alpha_2 < X_{\mathrm{HD}} < \alpha_1 \\ \alpha_2, & X_{\mathrm{HD}} \leqslant \alpha_2, \end{cases} \tag{9}$$

in which X_{HD} is given by Eq. (5). This model shows that the linearity range of HD is limited by $[\alpha_2, \alpha_1]$; otherwise HD output signals will be saturated to the limits. The limits α_1 and α_2 need to be calibrated in practice and they are dependent of homodyne detector electronics as mentioned. Due to homodyne detector saturation, variations of HD signals become much lower compared to the case in the linear detection region, which will affect the correctness of HD statistic measurements [28,29]. Moreover, when there is also the offset due to an imbalance imperfection on HD, it can significantly change the precalibrated linear detection ranges if the offset factor D_{LO} becomes comparable to α_1 or α_2, which needs to be further studied in experiments.

B. Experimental analysis on a practical homodyne detector

In order to study the influence of HD imbalance and electronics saturation on HD output signals, we design a simple experimental test of the HD shot-noise measurement.

We slightly modify the standard shot-noise measurement procedure and compare the results under different balancing settings. The key idea of this test is that we intentionally unbalance HD to study its influence on the HD saturation limit and further on HD output signals.

The experimental setup is shown in Fig. 1 where we only send LO pulses and then measure HD signals. We use a 1550-nm distributed feedback laser (Alcatel LMI1905) to first prepare a train of optical pulses with pulse widths of 100 ns and a repetition rate at 1 MHz as LO pulses. Our homodyne detector consists of two PDs (JDS Uniphase EPM 605), the AmpTek A250 as the first stage amplifier with a charge amplifier setting and a MAX4107 as the second stage amplifier. This HD features low noise (with a noise variance on the order of 10 mV^2) and a low bandwidth (about 10 MHz). We send LO pulses into port 2 of the homodyne detector (Fig. 1) and roughly minimize the HD output by adjusting the optical loss of one path in order to balance the HD, which is considered the first HD balance setting. After measuring the average optical power of the input pulses with a power meter, we then record HD signals over 1 s, which corresponds to 10^6 pulses. We adjust our DAQ system's (Model NI6111) detection range to $[-0.5 \text{ V}, 0.5 \text{ V}]$ as the detection limits. Any HD signals out of this range will be saturated to $\alpha_1 = 0.5$ V or $\alpha_2 = -0.5$ V. Note that this is not the saturation limit of our homodyne detector amplifier, which is about ± 3 V, but we want to limit the linear detection range to be small in order to highlight its influence on HD signals. Based on the measured 10^6 HD signals, we then estimate the mean and variance of this set of data, which is considered as one shot-noise measurement for a given LO intensity. With the same balance setting, we repeat this shot-noise measurement by gradually increasing the LO intensity. The experimental results for the first setting are shown as blue squares in Fig. 2. As shown in Fig. 2(a), the mean value first increases linearly with respect to LO intensity, which matches the prediction of Eq. (6). However, when the LO intensity reaches about 35 μw, the mean value stops increasing but saturates at 0.5 V. This is obviously due to the HD saturation effect predicted by Eq. (9) when the imbalance offset D_{LO} reaches the detection upper limit α_1. By applying Eq. (7) in Eq. (9) and fitting experimental data in the linear region, we successfully predict the behavior of the HD mean values as shown as the blue solid curve in Fig. 2(a).

Regarding the variance measurements, from Fig. 2(b) we can verify that the HD variance increases linearly with LO intensity, which matches the prediction of Eq. (7). Similarly, when the LO intensity reaches a relatively high value around 35 μw, the variance drops quickly and becomes zero at about 45 μw. This is because the HD signals variation becomes much lower when HD is saturated as any HD signal fluctuations beyond $\alpha_1 = 0.5$V have been cut off. We also observe that the HD variance does not immediately become zero, because only parts of the HD signals due to vacuum fluctuations have been limited by α_1 between a LO intensity of 35 and 45 μw. We use the saturation model [Eq. (9)] and shot-noise variance [Eq. (7)] to simulate HD variance behaviors as for the blue solid curve. As shown in Fig. 2(b), the simulation curve matches the behaviors of experimental HD variance data, which means we can account for the saturation model in further analysis.
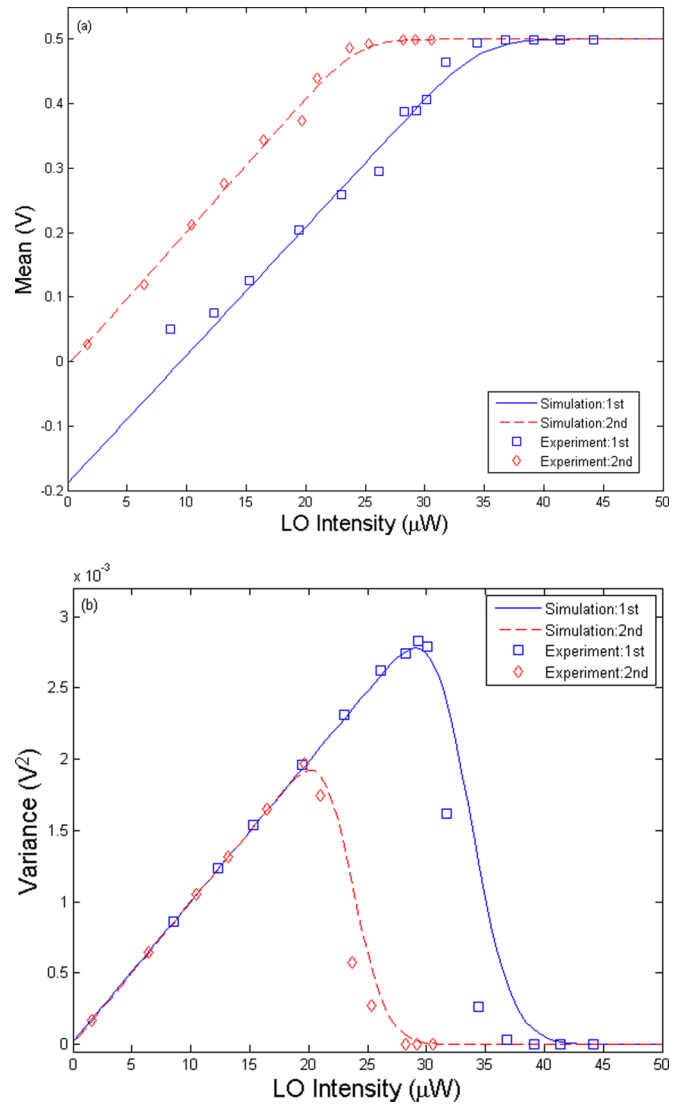

FIG. 2. Characterization of HD output voltage statistics, in the absence of signal, under two different balancing conditions (solid lines and dashed lines): (a) mean value V versus LO power and (b) variance V^2 versus LO power.

In order to illustrate the impact of HD imbalance on HD signals, we now slightly adjust the optical loss of one path after the BS to unbalance the HD. Such a balance setting (second) imposes more LO leakage, which will further affect the behaviors of the HD means and variances. With this balance setting, we repeat the HD statistic measurements mentioned above and compare them with previous results at the same LO intensity levels. Experimental and simulation results are shown as red diamonds and dashed curves in Fig. 2, respectively. As shown in Fig. 2(a), the HD mean under the second setting reaches a saturation limit around 35 μw compared to the one at 45 μw in the first setting. This confirms Eq. (7), in which the HD offset due to LO intensity leakage is proportional to ϵ and thus the equivalent displacements D_{LO} on HD signals of the second setting are larger than the one of the first setting. In consequence, the HD signal of the second setting reaches the detection limit α_1 at a smaller value of LO intensity compared

to the first setting, which can be observed by experimental (red diamonds) and simulation (red dashed curve) data in Fig. 2(b). The simulation curves also confirm the HD statistical behaviors, which shows that HD imbalance imperfections can influence the relation between HD saturation level and LO input intensity to a certain extent. Note that in CV QKD, HD is designed to precisely detect weak quantum signals; it can be saturated easily if the homodyne detector is not well balanced as the LO intensity is usually many orders of magnitude stronger than the quantum signal [43,44]. These experimental and simulation results inspire us to formalize a different attack strategy in CV QKD similar to blinding attack in DV QKD, where Eve inserts external light into the signal port of Bob's homodyne detector to influence HD output signals by taking advantage of the HD imbalance and saturation imperfections.

IV. HOMODYNE-DETECTOR-BLINDING ATTACK ON GMCS CV QKD

A. Principle of the attack

Based on the previous analysis, Eve can formalize a simple strategy to saturate Bob's HD output signal by sending another incoherent classical light into the HD's signal port instead of preparing coherent displacement as in a saturation attack [28,29]. Since Bob balances his HD with respect to the LO light that goes into the LO port, any relatively strong light going into the signal port cannot be subtracted as much as the one in LO port. Thus the external light contributes a strong offset on the HD output signal; at a certain point it can cause HD saturation as shown in the preceding section. In order to prevent inference with LO pulses, Eve can send the external light in a different mode of the LO pulse; in practice she can use a different wavelength other than the one used for LO pulses. Moreover, due to the BS's wavelength-dependent properties, Eve has the possibility to "control" the transmission of Bob's BS by selecting the proper wavelength of the external light [21,22,45]. On the other hand, the two PDs used in HD are classical detectors and usually have large wavelength ranges (typically from 800 to 1700 nm). Any light in the sensitive range of the PD can produce photocurrents and contribute to final HD signals, which makes it impossible for Alice and Bob to distinguish the source of light by only measuring HD signals. However, as Eve's external light is incoherent with Alice's

and Bob's LOs in CV QKD, the external light contributes excess noise into Alice's and Bob's HD measurements. On the other hand, such excess noise due to the external light can be "sufficiently filtered" by the LO pulses, in the sense that external light does not interfere with the LO and the related excess noise will be further normalized by a factor of N_0.

As mentioned, in order to break the security with current technologies, Eve can combine this strategy with the IR attack. If Bob's HD works in the linear region, Alice and Bob can always notice the excess noise due to Eve's IR attack and the external light. However, Eve can always cause Bob's HD signal saturation by sending strong enough external light. In this sense, Eve is able to control Bob's HD signals and manipulate the HD statistic measurements. If Eve carefully selects the properties of the external light, her manipulation of Bob's HD signals can further lead Alice and Bob to underestimate the excess noise from Eve's actions, which fully compromise the security. We will see in the following sections that such an attack strategy is simple to realize in experiments but is powerful enough for Eve to steal keys without being discovered.

B. Eve's attack strategy

By targeting a typical implementation of CV QKD [17], we now present Eve's homodyne detector-blinding attack strategy step by step along with a realistic implementation of Alice's and Bob's GMCS CV QKD protocols (a concept scheme of the attack strategy is shown in Fig. 3).

(i) In GMCS CV QKD, Alice prepares a quantum signal $|X + iP\rangle$ in which the amplitude X and phase P quadratures are continuously modulated with a bivariate centered Gaussian distribution (due to the symmetry of X and P, we will only look at the X quadrature in our analysis)

$$X = X_A + X_0, \qquad (10)$$

with a variance $V_A = \langle X_A^2 \rangle - \langle X_A \rangle^2$ and the vacuum noise $\langle X_0^2 \rangle = 1$.

(ii) Eve cuts down the quantum channel and performs a full IR attack [39]: Eve intercepts Alice's signals by performing heterodyne detection on X and P quadratures to obtain the
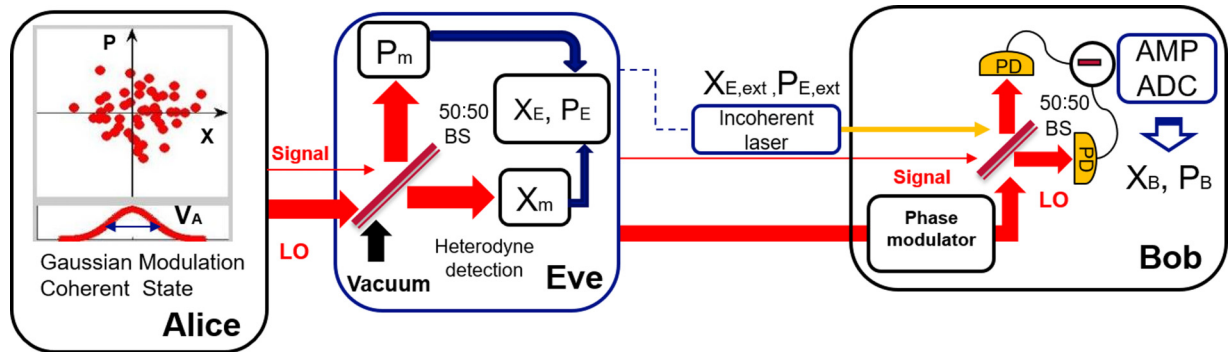

FIG. 3. Concept scheme of Eve's homodyne detector-blinding attack in CV QKD: Alice, preparation of the coherent state with Gaussian modulation V_A; Eve, heterodyne measurement X_M, P_M, re-preparation X_E, P_E, and external light state $X_{E,\text{ext}}, P_{E,\text{ext}}$; Bob, homodyne detector measurement X_B, P_B; BS, beam splitter; LO, local oscillator; PD, pin photodiode; AMP, amplifier; ADC, analog-to-digital converter.

measurement result

$$X_M = \frac{1}{\sqrt{2}}(X_A + X_0 + X_0'), \tag{11}$$

where, due to the BS in heterodyne detection, there is a factor $1/\sqrt{2}$ for loss and a vacuum state X_0' added. According to her measurements (X_M and P_M), Eve prepares and resends her noisy coherent states $|X_E + iP_E\rangle$ as signals to Bob through a lossy channel with transmission of T,

$$X_E = gX_M + X_0'' = \frac{g}{\sqrt{2}}(X_A + X_0 + X_0') + X_0'', \tag{12}$$

in which $g = \sqrt{2}$ is the gain factor to compensate for the loss due to heterodyne detection and X_0'' is a noise term due to coherent state encoding of Eve. In addition, X_0' and X_0'' both follow a centered normal distribution with unity variance.

(iii) Along with her resending signals, Eve inserts external laser pulses into the signal port of Bob's homodyne detector, which is not coherent with CV QKD signals. In practice, Eve needs to choose the properties of the external light: The wavelength is slightly different from Alice's signal, the pulse width and repetition rate are the same as Alice's signals, and the intensity or photons per pulse depend on how much Eve wants to influence Bob's homodyne detector measurement, which will be analyzed in the next section. In order to insert such pulses into Bob's homodyne detector, Eve can set the polarization of them as the ones of the CV QKD signals, if a polarization multiplexing technique is used [19].

(iv) Bob performs HD measurements on Eve's incoming signal pulses interfering with LO pulses and the external laser pulses interfering with the vacuum. Since the external laser pulses are incoherent with CV QKD signals, there is no interference between the external light and LO pulses; we can independently analyze the impact of the external laser and Eve's IR signals on Bob's HD output signals. Regarding HD with an ideal infinite detection range $(-\infty, \infty)$ and an efficiency of η, Bob's HD output signal can be given as

$$X_{Bi} = \sqrt{\eta I_{LO}}[\sqrt{\eta T}(X_E + X_{\text{tech}}) + \sqrt{1 - \eta T}X_0'''] \\ + X_{E,\text{ext}} + X_{\text{ele}}, \tag{13}$$

in which X_{tech} is the noise term due to any technical noises from Eve's, Alice's, and Bob's devices; X_0''' is another vacuum state due to loss in Bob's HD; and $X_{E,\text{ext}}$ is the external light state that impacts Bob's HD output, which can be treated as the case in which only LO pulses go into HD [Eq. (5) in Sec. III A]:

$$X_{E,\text{ext}} = \eta(1 - 2T_{\text{ext}})I_{\text{ext}} + 2\sqrt{\eta T_{\text{ext}}(1 - T_{\text{ext}})I_{\text{ext}}}X_0''''. \tag{14}$$

Here T_{ext} is the overall transmission of HD regarding the external light pulses that goes into a signal port, I_{ext} is the number of photons per external light pulse, and X_0'''' is the vacuum state that interferes with the external light. As Bob's HD balance setting is only valid for LO pulses going into the LO port, the overall imbalance factor $\epsilon_{\text{ext}} = 1 - 2T_{\text{ext}}$ of the external light pulses will contribute non-negligible offsets to final HD signals. The second term of Eq. (14) will contribute its own shot noise into the CV QKD excess noise. In a realistic case, Bob's HD only operates linearly with a finite detection range $[\alpha_2, \alpha_1]$, as discussed in Sec. III; thus Bob's HD output signal is given by Eq. (9) in which X_{Bi} [Eq. (13)] replaces the term of X_{HD}.

(v) Alice and Bob perform classical postprocessing on their correlated data (X_A and X_B), i.e., sifting, parameter estimation, reverse reconciliation, and privacy amplification, in order to obtain keys. Due to Eve's external light, Alice and Bob may believe their excess noise is still below the null threshold, which will cause them to accept compromised keys.

(vi) Eve listens to the classical communication between Alice and Bob in order to perform the same postprocessing of Alice and Bob on her data to get identical keys.

V. SECURITY ANALYSIS AND SIMULATIONS

In this section we will demonstrate a simulation of Eve's attack strategy in Sec. IV B and show how Eve can in practice break the security of Alice's and Bob's GMCS CV QKD systems with a realistic parameter setting.

A. Realistic assumptions of Alice, Bob, and Eve

In the security analysis, it is necessary to assume Alice and Bob's CV QKD implementation setups and Eve's power in a realistic scenario such that Eve's security breach can be valid. We first consider the assumptions of Alice and Bob's CV QKD implementations and their device parameters.

(a) Alice optimizes her Gaussian modulation variance $V_A \in \{1, 100\}$ based on the distance [33].

(b) Bob balances his HD on the LO pulses that go into the LO port such that $T_{LO} \approx 0.5$ and one LO pulse contains $I_{LO} = 10^8$ photons on Bob's side. Thus the impact of LO leakage on HD is assumed to be negligible.

(c) Alice and Bob implement real-time shot-noise calibration as in Ref. [19]; it is assumed that their shot noise $N_0 = \eta I_{LO}$ is not tampered with by Eve. Such an assumption can be extended to the case in which Alice and Bob use the LLO scheme [24]

(d) Bob's HD efficiency $\eta = 0.6$, electronic noise variance $v_{\text{ele}} = 0.01N_0$, and linear detection limit $\alpha_1 = -\alpha_2 = 20\sqrt{N_0}$. Such limits are considered large enough to ensure Bob's HD operating in the normal case. Alice and Bob calibrate η and v_{ele} before the CV QKD protocol.

(e) Alice and Bob perform reverse reconciliation with a reconciliation efficiency of 95%.

We now consider Eve's attack strategy assumptions.

(i) Eve's station is right after Alice's station. The loss between Alice and Bob is identical to the one between Eve and Bob, which is given by $T = 10^{-aL/10}$, where L is the distance between Alice and Bob and $a = 0.21$ dB/km is the standard loss coefficient of a single-mode fiber in 1550 nm.

(ii) Eve inserts the external light beside Bob's station such that Eve can control precisely its power I_{ext} without it going through the lossy channel.

(iii) Eve inserts the external light into Bob's homodyne detector signal port and its overall transmission on Bob's HD is $T_{\text{ext}} = 0.49$. Note that Eve is assumed to know T_{ext} and can control its value by using a shorter or longer wavelength as in the wavelength attack [21–23].

B. Eve's impact and excess noise contribution

Based on these assumptions, we can now analyze Eve's impact and excess noise contribution over Alice's and Bob's

CV QKD protocols. From Alice's and Bob's points of view, all the statistical quantities need to be normalized into shot-noise units, which will be considered in the following analysis. From Eve's strategy mentioned above, there are mainly three parts of excess noise due to Eve's attack: noise due to the IR attack ξ_{IR}, noise due to the external light ξ_{ext}, and noise due to technical imperfections ξ_{tech}. Since LO pulses and external light pulses are in different modes, we can separately evaluate ξ_{IR} and ξ_{ext}.

As in step (ii) of Eve's strategy, Eve's IR attack adds one vacuum noise due to the 50:50 BS in the heterodyne detection X_0' and another one due to coherent encoding X_0'', which gives $\xi_{IR} = 2$ [39]. We further consider the total technical noise due to Alice's, Bob's, and Eve's device imperfections as $\xi_{tech} = 0.1$, which is an experimental result in Ref. [39].

Regarding the noise due to the external light in steps (iii) and (iv) of Eve's strategy, as in the analysis in Sec. III A, there are mainly two parts: the external light's own shot noise $N_{0,ext}$ and the laser intensity fluctuation noise $V_{f,ext}$ due to insufficient subtraction of Bob's HD. If we further express these values into shot-noise units with ηI_{LO}, we can know their excess noise contributions

$$N_{0,ext} = 4T_{ext}(1 - T_{ext})I_{ext}/I_{LO}, \tag{15}$$

$$V_{f,ext} = \eta f_{ext}^2(1 - 2T_{ext})^2 I_{ext}^2/I_{LO} \tag{16}$$

in which f_{ext} is the external laser's intensity fluctuation ratio; we consider that Eve has an ultrastable laser source $f_{ext} = 0.1\%$ or a normal laser source $f_{ext} = 2\%$. Thus the total noise due to Eve's external light is given by

$$V_{B2} = N_{0,ext} + V_{f,ext} \tag{17}$$

$$= 4T_{ext}(1 - T_{ext})R + R^2\eta f_{ext}^2(1 - 2T_{ext})^2 I_{LO}, \tag{18}$$

in which $R = I_{ext}/I_{LO}$ is the ratio between the photon number of one of Eve's external light pulses and one of Bob's LO pulses. Note that V_{B2} is the noise due to external light on Bob's side; the equivalent noise of V_{B2} on Alice's side needs to take the transmission T into account. Thus the total excess noise due to the external light is given as

$$\xi_{ext} = 4T_{ext}(1 - T_{ext})R/T + R^2\eta f_{ext}^2(1 - 2T_{ext})^2 I_{LO}/T. \tag{19}$$

We summarize all these noises due to Eve's attack in Fig. 4. As we can see, $N_{0,ext}$ and $V_{f,ext}$ due to the external laser increase with I_{ext}. If Eve uses a stable laser source as her external light with $f_{ext} = 0.1\%$, the dominant noise contribution is from its shot noise $N_{0,ext}$. However, if Eve uses a common laser source with $f_{ext} = 2\%$, the intensity fluctuation noise $V_{f,ext}$ will take the lead and induce more disturbances on CV QKD signals, which needs to be considered in practice. In our later analysis, we will consider $f_{ext} = 0.1\%$ in Eve's attack. We can also observe that Eve's external light noise increases with Alice's and Bob's distance L due to the factor of $1/T$, as the external light is inserted on Bob's side. On the other hand, Eve's external light also contributes a non-negligible offset on Bob's HD output signal as discussed in Sec. III A, which is under Eve's control through T_{ext} and I_{ext}:

$$D_{ext} = \sqrt{\eta/I_{LO}}(1 - 2T_{ext})I_{ext} = R\sqrt{\eta I_{LO}}(1 - 2T_{ext}). \tag{20}$$
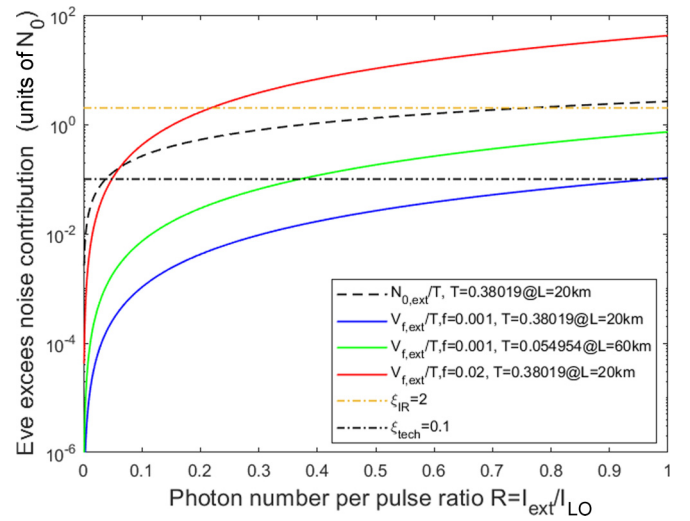

FIG. 4. Excess noise contributions, for different blinding attack parameters, as a function of the photon number per pulse ratio R. Solid curves stand for the excess noise due to the blinding laser intensity fluctuation (see the text). The dashed curve stands for excess noise added by blinding laser shot noise. The upper dash-dotted line stands for the excess noise due to the IR attack and the lower dash-dotted line stands for the technical excess noises, which are independent of the external blinding laser.

Note that D_{ext} is normalized in $\sqrt{N_0}$. Since D_{ext} is proportional to I_{ext}, if Eve wants more influence from external light on Bob's HD, she needs to increase ξ_{ext}, which may potentially limit the power of the attack. In order to achieve a security breach, Eve needs to properly set D_{ext} in order to cause a large enough offset to force Bob's HD to work in the saturation region, which will help Eve to effectively bias the noises ξ_{IR}, ξ_{ext}, and ξ_{tech} due to the attack.

C. Alice's and Bob's parameter estimations under Eve's attack

In order to determine whether Eve can have a security breach under the homodyne detector-blinding attack, we need to evaluate the parameter estimations of Alice and Bob for channel transmission $\hat{T}$ and excess noise $\hat{\xi}$ to see whether Eve can bias the excess noise due to an attack small enough such that Alice and Bob believe they can still share a secret key. A security breach thus corresponds to the condition $\hat{\xi} < \xi_{null}$, in which ξ_{null} is the null key threshold that corresponds to the maximum excess noise that allows Alice and Bob to extract a secret key under collective attack model [35] for given values of $\hat{T}$ and V_A. According to the standard parameter estimation procedure of CV QKD in Sec. II A, we can estimate $\hat{T}$ and $\hat{\xi}$ based on Eqs. (2) and (3).

We first consider the case where Bob's HD linear range is infinite $(-\infty, \infty)$. In this case, we can predict the mean of Bob's HD measurement $\langle X_{Bi} \rangle = D_{ext}$ and its variance

$$V_{Bi} = \langle X_{Bi}^2 \rangle - \langle X_{Bi} \rangle^2 \tag{21}$$

$$= \eta T(V_A + \xi_{IR} + \xi_{ext} + \xi_{tech}) + 1 + v_{ele}, \tag{22}$$

in which we can directly deduce the channel transmission estimation of Alice and Bob, $\hat{T}_i = T$, and their excess noise estimation $\hat{\xi}_i = \xi_{IR} + \xi_{tech} + \xi_{ext}$. It is obvious that Alice and

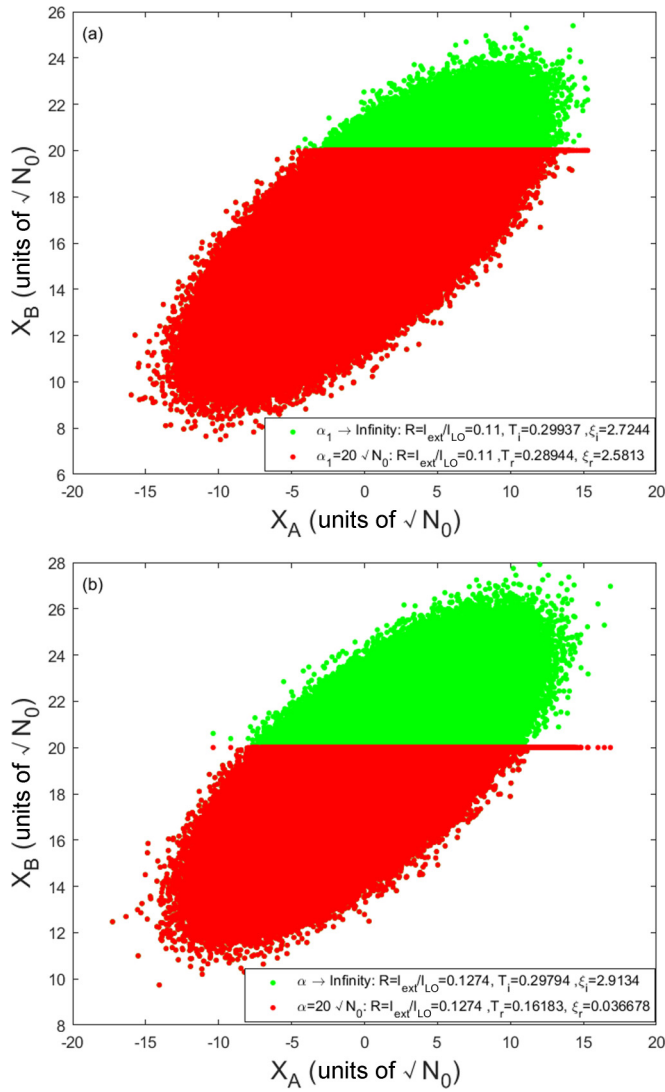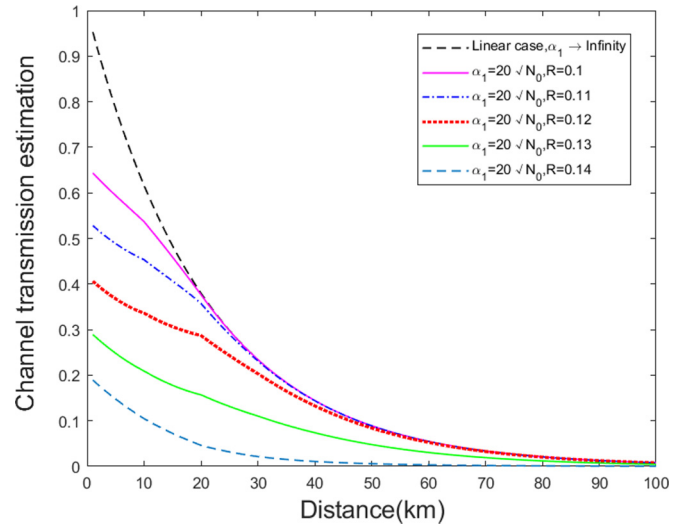FIG. 6. Alice and Bob's transmission estimation versus distance under Eve's homodyne detector-blinding attack. The black dashed curve (top one) corresponds to $\hat{T}_i$, which is estimated by X_{Bi} in the linear case, while the other lower curves correspond to the $\hat{T}_r$ in the realistic case, which are estimated by X_B with $R = 0.1, 0.11, 0.12, 0.13, 0.14$ from top to bottom.

FIG. 5. Simulation of the impact of detector saturation on the quadratures distribution X_B versus X_A, for two sets of parameters: (a) $R = 0.11$, with no security breach as $\hat{\xi}_r \gg \xi_{null}$, and (b) $R = 0.1274$, with a security breach as $\hat{\xi}_r < \xi_{null}$. For both cases, $\hat{\xi}_i \gg \xi_{null}$. Red (dark gray) shows the X_B HD detection range $[-20\sqrt{N_0}, 20\sqrt{N_0}]$ and green (light gray) the X_{Bi} HD ideal linear case. The corresponding estimation of $\hat{T}$ and $\hat{\xi}$ is given in the legend for X_B and X_{Bi}, respectively.

Bob can easily spot Eve's attack action if Bob's HD works in the linear region, as $\hat{\xi}_i \gg \xi_{null}$ at any distances. However, if Bob performs a realistic HD measurement with a finite linear range $[\alpha_2, \alpha_1]$, Eve can manipulate Bob's HD signal statistics by controlling D_{ext} through R, which affects Bob's HD output statistics and further biases Alice's and Bob's parameter estimations. We now demonstrate Eve's action on R and its impact on Alice and Bob's data (X_A and X_B) in simulation. As shown in Figs. 5(a) and 5(b), Eve uses $R = 0.1$ and $R = 0.1274$, respectively, in her strategy at a distance $L = 25$ km, in which (X_A, X_{Bi}) (green or light gray) corresponding to Bob's HD linear range is infinite ($-\infty, \infty$) and (X_A, X_B) (red or dark gray) corresponding to Bob's HD is limited to $[\alpha_2, \alpha_1]$. If Alice and Bob perform parameter

estimation based on (X_A, X_{Bi}), where only a displacement D_{ext} has been introduced on Bob's data, they can still notice Eve's attack based on $\hat{T}_i$ and $\hat{\xi}_i$. However, Alice and Bob may not be able to detect Eve's action based on (X_A, X_B), as Eve can gradually increase R in order to force parts of Bob's HD signals to be saturated and bias the estimation of $\hat{T}_r$ and $\hat{\xi}_r$. Due to Bob's HD saturation, the X_B variation is limited by Bob's upper detection limit $\alpha_2 = 20$, which results in the smaller variance for Bob compared to the one of X_{Bi} and a weaker covariance correlation between Alice and Bob, which leads $\hat{T}_r < \hat{T}_i$. If Eve chooses properly the value of R, she can eventually meet the condition $\hat{\xi}_r < \xi_{null}$. In Fig. 5(a) Eve's choice of $R = 0.1$ cannot lead to a security breach as $\hat{\xi}_r = 2.5813 > \xi_{null} = 0.1013$ at 25 km. If Eve keeps increasing I_{ext}, as shown in Fig. 5(b), the choice of $R = 0.1274$ corresponds to a security breach condition as $\hat{\xi}_r = 0.0367 < \xi_{null}$. In Fig. 5, statistical measurements are based on the $N = 10^7$ simulation data for linear HD (green or light gray) and the saturation HD case (red or dark gray). This shows that Eve's external light power needs to be high enough to affect sufficiently Bob's data distribution in order to achieve a security breach; otherwise Alice and Bob can still detect the noise due to Eve's attack.

We further analyze Eve's choice of R to meet the condition $\hat{\xi}_r < \xi_{null}$. In the simulation of Eve's attack, we use the HD model in Sec. III A and the standard parameter estimation procedure of CV QKD in Sec. II A to estimate $\hat{T}_r$ and $\hat{\xi}_r$ for Alice and Bob. In particular, we calculate $\hat{T}_r$ and $\hat{\xi}_r$ by increasing the value of I_{ext} and thus the ratio R. In Fig. 6 we show the impact of R on $\hat{T}_r$ over the distance $L = 0 \sim 100$ km. As shown in Fig. 6, Eve's external light reduces Alice's and Bob's channel transmission $\hat{T}_r$ as expected; however, such a reduction will not prevent Alice and Bob from proceeding to key generation. As long as $\hat{\xi}_r < \xi_{null}$, there is still a security breach. To illustrate Eve's impact on Alice's and Bob's estimations of
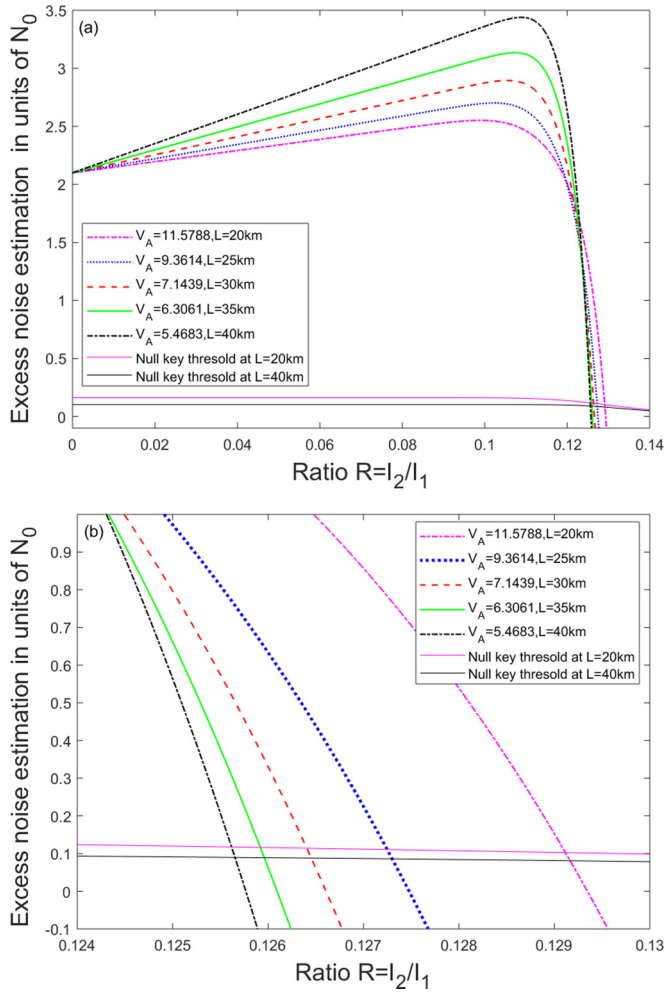
FIG. 7. Excess noise estimation of Alice and Bob versus photon number ratio R, with $\eta = 0.55$, $T_{ext} = 0.49$, $f_{ext} = 0.1\%$, and $v_{ele} = 0.01$, for the range of R equal to (a) 0–0.14 and (b) 0.124–0.13. The five upper curves stand for the excess noise estimations $\hat{\xi}_r$ at different distances and the two lower curves stand for the null key thresholds ξ_{null} at 20 and 40 km.

$\hat{\xi}_r$, we continuously increase R and deduce the corresponding $\hat{\xi}_r$ and ξ_{null} for a given setting of V_A and $\hat{T}_r$. The results of $\hat{\xi}_r$ and ξ_{null} versus R are shown in Fig. 7 for different distances $L = 20$, 25, 30, 35, and 40 km, in which excess noise $\hat{\xi}_r$ in the HD linear region increases with R and with distance due to the factor of $\hat{T}_r$. According to the previous analysis, Eve's noises consist of constant noises, i.e., 0.1 due to technical imperfections and 2 due to IR attack, and variable noises increasing with R, i.e., the shot noise of the external laser and its intensity fluctuation noise. The total noise is much higher than the tolerable excess noise for Alice and Bob to generate a key ($\xi_{null} \sim 10\% N_0$) and thus it will reveal Eve's presence.

However, $\hat{\xi}_r$ decreases sharply when $R > 0.12$, since the corresponding offset D_{ext} exceeds the HD detection limit α_1 such that $\hat{\xi}_r$ is effectively biased by Eve. As shown in the previous analysis, due to HD saturation, Bob's HD variance and his data's covariance with Alice both become smaller. However, the impact of HD saturation on its variance degradation is much larger than on the covariance, which results in a quick drop of

$\hat{\xi}_r$. Although the curves in Fig. 7(a) sharply decrease around $R = 0.12$, each value of $\hat{\xi}_r$ only corresponds to one value of R. As shown in Fig. 7(b), a more precise control of R will help Eve manipulate $\hat{\xi}_r$ to an arbitrary value between 0 and ξ_{null}. This means that once Eve has enough precision on the power of the external laser, she can accurately manipulate Alice's and Bob's excess noise estimations to any small value she desires. For example, according to the simulations, a successful attack is possible with the choice of $I_{ext} = R I_{LO} = 0.1274 \times 10^8 = 1274 \times 10^4$ and $f_{ext} I_{ext} = 1274$, which shows that Eve needs a precision of 10^4 photons and a stability of 10^3 photons level on one external laser pulse in order to accurately bias the excess noise estimation. Such precision is realistic and achievable with current technology.

For a given distance, Eve can in practice choose a proper value of R to achieve $\hat{\xi}_r < \xi_{null}$ such that Alice and Bob still believe they share a secure key according to their parameter estimation and proceed to key generation; however, the generated keys are not secure at all because of Eve's IR attack. In principle, Eve can set $\hat{\xi}_r$ to be arbitrarily close to zero, which further enables her to control Alice's and Bob's key rate generation. Figure 7 is a reference for Eve to properly set the value of R.

VI. COUNTERMEASURES

In DV QKD, a blinding attack is well known for breaking security on various protocols through controlling different types of SPDs such as the avalanche photodiode (APD) [6,8] and superconducting nanowire SPD [46,47]. This kind of detector-controlled attack based on bright illumination now extends to CV QKD using HD as shown in this paper. In both the CV and the DV case, Eve is required to send a relatively strong classical light to actively control Bob's detector. Due to such similarity, countermeasures against blinding attack in DV QKD are thus worth considering to defeat the HD-blinding attack in CV QKD. Here we briefly discuss several possible countermeasures against the homodyne detector-blinding attack in CV QKD and compare them with the ones in DV QKD.

In the first approach, a straightforward countermeasure is to monitor the light intensity that is going into the signal port of homodyne detector. Bob can implement such a countermeasure using a sensitive p-i-n photodiode, in order to detect any strong light impinging on the signal port. Such a method can be used also for the energy test that is required in some security proofs [37]. It is however challenging to build a detection system that can give in practice the capability to detect light in any optical mode that Eve may try to use. In DV QKD, such watchdog detectors have been proposed [9] and implemented [48] to detect a blinding attack. However, it has been shown that a practical watchdog may not always be able to raise the alarm [49]. Moreover, Eve may also use a high-power laser to damage the photodiode watchdog and bypass the security alarm of the QKD protocol [50].

Bob's homodyne detector consists of two classical photodiodes (PDs). Hence, instead of measuring the difference between the two photocurrents, Bob may also monitor one, or the sum of the two photocurrents, from two PDs. This may be challenging in practice, however, as it will disturb the HD output and it can be difficult to set a proper discrimination level

to correctly detect against a blinding attack. In our proposed blinding attack strategy, Eve only needs to increase the overall energy by about 12%. Hence LO intensity fluctuations, due to Alice's laser source and channel environment, may exceed the external light's energy, which can lead to false alarms. In addition, it is currently technically challenging to design a high-gain, high-bandwidth, high-efficiency, low-noise homodyne detector in practice for CV QKD purposes. Adding extra electronic components can increase the electronic noises and reduce HD performance. A similar approach in DV QKD has been also proposed, in which Bob monitors the photocurrent from the APD [51]. Unfortunately, such a method was later proven insufficient to detect the blinding attack in many particular cases [11]. Moreover, in addition to monitoring the photocurrent from the APD, one may use the synchronization detector as an auxiliary monitor to detect the blinding light [52].

Another countermeasure has been proposed in the Ref. [53]: Alice and Bob test the linearity between the noise and signal measurement by using an active attenuation device on Bob's side, i.e., an amplitude modulator. Such a method explores the linearity of HD and can thus in principle prevent the homodyne detector-blinding attack: The randomization of the signal port's attenuation prevents Eve from properly setting the intensity of blinding pulses. However, a practical amplitude modulator is wavelength sensitive, which can lose its amplitude extension when the wavelength is out of the spectral range. In addition, such a linearity test increases the implementation complexity and detector losses. A similar approach, based on random detector efficiency, has also been proposed in DV QKD [54], yet it has been shown that it is not always effective in a practical implementation [10].

The three previous approaches require some modifications to the CV QKD system hardware, leading to additional experimental complexity. We suggest, on the other hand, that data postprocessing combined with calibrated homodyne detection can be a simple and efficient way to counter the blinding attack. We propose the following generic method. Bob sets security thresholds $[S_2, S_1]$ inside the HD limits $[\alpha_2, \alpha_1]$. In the parameter estimation stage, Alice and Bob can thus estimate, for each block, the fraction of the HD measurement data that have been recorded outside the interval $[S_2, S_1]$. If a too large fraction of HD measurements is recorded beyond the thresholds, then Alice and Bob know the HD was not working in its linear range for some non-negligible fraction of the quantum communication phase and they discard the block. This approach relies on the precalibration of homodyne detector detection limits (the values of α_1 and α_2) which is required to be performed with good precision (compared to N_0) and in a safe environment. Setting the value of the confidence interval $[S_2, S_1]$ and the fraction of rejected data that can be tolerated will require further work taking finite-size effects into account and including a characterization of statistical fluctuations.

Finally, since the homodyne detector-blinding attack is a detector-based attack, MDI CV QKD [55–57] can be a

potential solution to defeat such an attack. Although a proof-of-principle demonstration of MDI CV QKD has already been performed in experiment [57], there is still a large gap between practical implementation and the theoretical proposal. There are even debates on whether MDI CV QKD can become practical regarding its theoretical performance limitations and current available technologies [58,59]. Recent works in finite-size [60] and composable [61] security proofs of MDI CV QKD have shown some practical feasibilities of such protocol from theoretical perspectives. This paper may provide additional motivation for future development of practical MDI CV QKD, similarly to the role played by the blinding attack in DV QKD, to trigger the birth of MDI QKD [12,13] and its deployment [62].

These countermeasures show that current CV QKD implementations need some upgrades in hardware or software to defeat the proposed attack. It is even more important to verify the functionality of these countermeasures in practice, as they may fail to defeat the attacks if they are not correctly implemented as in the cases of DV QKD [10,11].

VII. CONCLUSION

In this paper we detailed an attack strategy exploiting the homodyne detection vulnerability [28,29] that is moreover implementable with low experimental complexity. Inspired by and analogous to the blinding attack in DV QKD, our attack allows Eve to influence Bob's homodyne detection response, by sending external light. We demonstrated that this attack can constitutes a powerful strategy that can fully break the security of practical CV QKD systems. Based on experimental observations, we proposed an effective model to account for homodyne detection imperfections and used it to model Eve's attack. Simulation results illustrate the feasibility of our proposed attack under realistic experimental conditions. Compared to other side channel attacks in CV QKD requiring complex experimental techniques [22,23,28], we believe our strategy should be simple enough to allow an effective eavesdropping demonstration on deployed CV QKD. This attack hence highlights the importance of exploring the assumptions in security proofs when implementing CV QKD protocols and the necessity to implement suitable countermeasures to ensure the practical security of CV QKD systems.

[1] V. Scarani, H. Bechmann-Pasquinucci, N. J. Cerf, M. Dušek, N. Lütkenhaus, and M. Peev, Rev. Mod. Phys. **81**, 1301 (2009).

[2] N. Gisin, G. Ribordy, W. Tittel, and H. Zbinden, Rev. Mod. Phys. **74**, 145 (2002).

[3] B. Qi, C.-H. F. Fung, H.-K. Lo, and X. Ma, Quantum Inf. Comput. **7**, 73 (2007).

[4] Y. Zhao, C.-H. F. Fung, B. Qi, C. Chen, and H.-K. Lo, Phys. Rev. A **78**, 042333 (2008).

[5] C. Wiechers, L. Lydersen, C. Wittmann, D. Elser, J. Skaar, C. Marquardt, V. Makarov, and G. Leuchs, New J. Phys **13**, 013043 (2011).

[6] V. Makarov, New J. Phys. **11**, 065003 (2009).

[7] S. Sajeed, P. Chaiwongkhot, J.-P. Bourgoin, T. Jennewein, N. Lütkenhaus, and V. Makarov, Phys. Rev. A **91**, 062301 (2015).

[8] L. Lydersen, C. Wiechers, C. Wittmann, D. Elser, J. Skaar, and V. Makarov, Nat. Photon. **4**, 686 (2010).

[9] I. Gerhardt, Q. Liu, A. Lamas-Linares, J. Skaar, C. Kurtsiefer, and V. Makarov, Nat. Commun. **2**, 349 (2011).

[10] A. Huang, S. Sajeed, P. Chaiwongkhot, M. Soucarros, M. Legré, and V. Makarov, IEEE J. Quantum Electron. **52**, 1 (2016).

[11] L. Lydersen, C. Wiechers, C. Wittmann, D. Elser, J. Skaar, and V. Makarov, Nat. Photon. **4**, 801 (2010).

[12] H.-K. Lo, M. Curty, and B. Qi, Phys. Rev. Lett. **108**, 130503 (2012).

[13] S. L. Braunstein and S. Pirandola, Phys. Rev. Lett. **108**, 130502 (2012).

[14] C. Weedbrook, S. Pirandola, R. García-Patrón, N. J. Cerf, T. C. Ralph, J. H. Shapiro, and S. Lloyd, Rev. Mod. Phys. **84**, 621 (2012).

[15] J. Lodewyck, M. Bloch, R. García-Patrón, S. Fossier, E. Karpov, E. Diamanti, T. Debuisschert, N. J. Cerf, R. Tualle-Brouri, S. W. McLaughlin, and P. Grangier, Phys. Rev. A **76**, 042305 (2007).

[16] S. Fossier, E. Diamanti, T. Debuisschert, A. Villing, R. Tualle-Brouri, and P. Grangier, New J. Phys. **11**, 045023 (2009).

[17] P. Jouguet, S. Kunz-Jacques, A. Leverrier, P. Grangier, and E. Diamanti, Nat. Photon. **7**, 378 (2013).

[18] R. Kumar, H. Qin, and R. Alléaume, New J. Phys. **17**, 043027 (2015).

[19] P. Jouguet, S. Kunz-Jacques, and E. Diamanti, Phys. Rev. A **87**, 062313 (2013).

[20] X.-C. Ma, S.-H. Sun, M.-S. Jiang, M. Gui, Y.-L. Zhou, and L.-M. Liang, Phys. Rev. A **89**, 032310 (2014).

[21] X.-C. Ma, S.-H. Sun, M.-S. Jiang, and L.-M. Liang, Phys. Rev. A **87**, 052309 (2013).

[22] J.-Z. Huang, C. Weedbrook, Z.-Q. Yin, S. Wang, H.-W. Li, W. Chen, G.-C. Guo, and Z.-F. Han, Phys. Rev. A **87**, 062329 (2013).

[23] J.-Z. Huang, S. Kunz-Jacques, P. Jouguet, C. Weedbrook, Z.-Q. Yin, S. Wang, W. Chen, G.-C. Guo, and Z.-F. Han, Phys. Rev. A **89**, 032304 (2014).

[24] B. Qi, P. Lougovski, R. Pooser, W. Grice, and M. Bobrek, Phys. Rev. X **5**, 041009 (2015).

[25] D. B. S. Soh, C. Brif, P. J. Coles, N. Lütkenhaus, R. M. Camacho, J. Urayama, and M. Sarovar, Phys. Rev. X **5**, 041010 (2015).

[26] D. Huang, P. Huang, D. Lin, C. Wang, and G. Zeng, Opt. Lett. **40**, 3695 (2015).

[27] A. Marie and R. Alléaume, Phys. Rev. A **95**, 012316 (2017).

[28] H. Qin, R. Kumar, and R. Alléaume, *Proceedings of Emerging Technologies in Security and Defence*, SPIE Proc. Vol. 8899 (SPIE, Bellingham, 2013), p. 7.

[29] H. Qin, R. Kumar, and R. Alléaume, Phys. Rev. A **94**, 012325 (2016).

[30] F. Grosshans and P. Grangier, Phys. Rev. Lett. **88**, 057902 (2002).

[31] F. Grosshans, G. Van Assche, J. Wenger, R. Brouri, N. J. Cerf, and P. Grangier, Nature (London) **421**, 238 (2003).

[32] E. Diamanti and A. Leverrier, Entropy **17**, 6072 (2015).

[33] P. Jouguet, S. Kunz-Jacques, and A. Leverrier, Phys. Rev. A **84**, 062317 (2011).

[34] R. García-Patrón and N. J. Cerf, Phys. Rev. Lett. **97**, 190503 (2006).

[35] M. Navascués, F. Grosshans, and A. Acín, Phys. Rev. Lett. **97**, 190502 (2006).

[36] A. Leverrier, Phys. Rev. Lett. **114**, 070501 (2015).

[37] A. Leverrier, Phys. Rev. Lett. **118**, 200501 (2017).

[38] P. Jouguet, S. Kunz-Jacques, E. Diamanti, and A. Leverrier, Phys. Rev. A **86**, 032309 (2012).

[39] J. Lodewyck, T. Debuisschert, R. García-Patrón, R. Tualle-Brouri, N. J. Cerf, and P. Grangier, Phys. Rev. Lett. **98**, 030503 (2007).

[40] R. Kumar, E. Barrios, A. MacRae, E. Cairns, E. Huntington, and A. Lvovsky, Opt. Commun. **285**, 5259 (2012).

[41] Y.-M. Chi, B. Qi, W. Zhu, L. Qian, H.-K. Lo, S.-H. Youn, A. I. Lvovsky, and L. Tian, New J. Phys. **13**, 013003 (2011).

[42] A. R. Williams, A. L. Kellner, X. S. Jiang, and P. K. L. Yu, Electron. Lett **28**, 2258 (1992).

[43] Y. Chi, High speed homodyne detector for Gaussian-modulated coherent-state quantum key distribution, Ph.D. thesis, University of Toronto, 2009 .

[44] S. Fossier, Mise en oeuvre et évaluation de dispositifs de cryptographie quantique à longueur d'onde télécom, Ph.D. thesis, Université de Paris–Sud, 2009.

[45] H.-W. Li, S. Wang, J.-Z. Huang, W. Chen, Z.-Q. Yin, F.-Y. Li, Z. Zhou, D. Liu, Y. Zhang, G.-C. Guo, W.-S. Bao, and Z.-F. Han, Phys. Rev. A **84**, 062308 (2011).

[46] L. Lydersen, M. K. Akhlaghi, A. H. Majedi, J. Skaar, and V. Makarov, New J. Phys. **13**, 113042 (2011).

[47] L. Lydersen, N. Jain, C. Wittmann, O. Marøy, J. Skaar, C. Marquardt, V. Makarov, and G. Leuchs, Phys. Rev. A **84**, 032320 (2011).

[48] A. R. Dixon, J. F. Dynes, M. Lucamarini, B. Fröhlich, A. W. Sharpe, A. Plews, W. Tam, Z. L. Yuan, Y. Tanizawa, H. Sato, S. Kawamura, M. Fujiwara, M. Sasaki, and A. J. Shields, Sci. Rep. **7**, 1978 (2017).

[49] S. Sajeed, I. Radchenko, S. Kaiser, J.-P. Bourgoin, A. Pappa, L. Monat, M. Legré, and V. Makarov, Phys. Rev. A **91**, 032326 (2015).

[50] V. Makarov, J.-P. Bourgoin, P. Chaiwongkhot, M. Gagné, T. Jennewein, S. Kaiser, R. Kashyap, M. Legré, C. Minshull, and S. Sajeed, Phys. Rev. A **94**, 030302 (2016).

[51] Z. L. Yuan, J. F. Dynes, and A. J. Shields, Nat. Photon. **4**, 800 (2010).

[52] S. Wang *et al.*, Opt. Express **22**, 21739 (2014).

[53] S. Kunz-Jacques and P. Jouguet, Phys. Rev. A **91**, 022307 (2015).

[54] C. Lim, N. Walenta, M. Legre, N. Gisin, and H. Zbinden, IEEE J. Sel. Top. Quantum Electron. **21**, 1 (2015).

[55] Z. Li, Y.-C. Zhang, F. Xu, X. Peng, and H. Guo, Phys. Rev. A **89**, 052301 (2014).

[56] X.-C. Ma, S.-H. Sun, M.-S. Jiang, M. Gui, and L.-M. Liang, Phys. Rev. A **89**, 042335 (2014).

[57] S. Pirandola, C. Ottaviani, G. Spedalieri, C. Weedbrook, S. L. Braunstein, S. Lloyd, T. Gehring, C. S. Jacobsen, and U. L. Andersen, Nat. Photon. **9**, 397 (2015).

[58] F. Xu, M. Curty, B. Qi, L. Qian, and H.-K. Lo, Nat. Photon. **9**, 772 (2015).

[59] S. Pirandola, C. Ottaviani, G. Spedalieri, C. Weed-brook, S. L. Braunstein, S. Lloyd, T. Gehring, C. S. Jacobsen, and U. L. Andersen, Nat. Photon. **9**, 773 (2015).

[60] P. Papanastasiou, C. Ottaviani, and S. Pirandola, Phys. Rev. A **96**, 042332 (2017).

[61] C. Lupo, C. Ottaviani, P. Papanastasiou, and S. Pirandola, Phys. Rev. A **97**, 052327 (2018).

[62] H.-L. Yin, T.-Y. Chen, Z.-W. Yu, H. Liu, L.-X. You, Y.-H. Zhou, S.-J. Chen, Y. Mao, M.-Q. Huang, W.-J. Zhang, H. Chen, M. J. Li, D. Nolan, F. Zhou, X. Jiang, Z. Wang, Q. Zhang, X.-B. Wang, and J.-W. Pan, Phys. Rev. Lett. **117**, 190501 (2016).